Anticancer Agents Hot Paper

International Edition: DOI: 10.1002/anie.201602814
German Edition: DOI: 10.1002/ange.201602814

Cyclometalated Palladium(II) N-Heterocyclic Carbene Complexes: Anticancer Agents for Potent In Vitro Cytotoxicity and In Vivo Tumor Growth Suppression

*Tommy Tsz-Him Fong, Chun-Nam Lok, Clive Yik-Sham Chung, Yi-Man Eva Fung, Pui-Keong Chow, Pui-Ki Wan, and Chi-Ming Che**

Abstract: *Palladium(II) complexes are generally reactive toward substitution/reduction, and their biological applications are seldom explored. A new series of palladium(II) N-heterocyclic carbene (NHC) complexes that are stable in the presence of biological thiols are reported. A representative complex, [Pd(C^N^N)(N,N′-nBu$_2$NHC)](CF$_3$SO$_3$) (**Pd1 d**, HC^N^N = 6-phenyl-2,2′-bipyridine, N,N′-nBu$_2$NHC = N,N′-di-n-butylimidazolylidene), displays potent killing activity toward cancer cell lines (IC_{50} = 0.09–0.5 μM) but is less cytotoxic toward a normal human fibroblast cell line (CCD-19Lu, IC_{50} = 11.8 μM). In vivo anticancer studies revealed that **Pd1 d** significantly inhibited tumor growth in a nude mice model. Proteomics data and in vitro biochemical assays reveal that **Pd1 d** exerts anticancer effects, including inhibition of an epidermal growth factor receptor pathway, induction of mitochondrial dysfunction, and antiangiogenic activity to endothelial cells.*

There has been a growing interest in expanding the horizon of applications of palladium complexes besides catalysis.[1] In this regard, palladium(II) complexes have recently been examined as potential chemotherapeutic agents against cancer.[2] However, palladium(II) complexes that exhibit good in vivo anticancer activities remain to be explored. The main challenge for the development of anticancer palladium(II) complexes is their high reactivities toward sulfur-containing biomolecules, such as glutathione (GSH), and ease of substitution reactions under physiological conditions, leading to low in vivo stability and multiple speciation that complicates the potential therapeutic applications. Most of the reported palladium(II) complexes showed DNA-binding properties and IC_{50} values in the 10^{-5} to 10^{-3} M range. Palladium(II) complexes showing antiproliferative properties with molecular target(s) other than DNA remain underdeveloped. Considerable evidence shows that cytotoxic metal complexes that inhibit the activities of enzymes, such as histone deacetylase, telomerase, topoisomerase, thioredoxin reductase, and protein kinases, could be effective for treatment of cancers, including those with drug-resistance.[3]

Developing physiologically stable anticancer metal complexes is advantageous because speciation, which affects the biological activities and pharmacokinetic properties of such complexes, could be minimized. Introducing strong metal–carbon bonds and multidentate ligands serves as an effective way to suppress demetalation of the metal complexes. The NHC moiety is a strong σ-donor ligand that can form stable metal–$C_{carbene}$ bonds with most transition-metal ions. Moreover, the NHC ligand itself is relatively non-toxic, and versatile structures of NHC can be easily prepared.[4,5] Together with the improved stability provided by the chelating effect of tridentate pincer ligands, herein we report a series of anticancer cyclometalated palladium(II) complexes containing NHC ligands, $[Pd(C^N^N)(NHC)]^+$, which are stable in the presence of biological thiols. Proteomics and subsequent biochemical assays revealed that the complexes induce mitochondrial dysfunction and inhibit the cancer promoting epidermal growth factor receptor pathway.

Cyclometalated palladium(II) complexes containing NHC ligands with different alkyl chain lengths were prepared (**Pd1 a**–**Pd1 d**; Figure 1; see the Supporting Information for experimental details and characterization data). In general, a mixture of [Pd(C^N^N)Cl] and the corresponding NHC ligand in the presence of KO*t*Bu was heated under reflux for 24 h to give palladium(II) NHC complexes, after purification by column chromatography and recrystallization. The complexes were characterized by elemental analyses, FAB-MS spectrometry, and ^{1}H, ^{19}F, and ^{31}P NMR spectroscopy (Supporting Information). Other palladium(II) complexes, **Pd2 a**, **PdPPh$_3$**, **Pdiso,** *trans*-[Pd(NHC)$_2$Cl$_2$], and [Pd(C^N^N)Cl], were also prepared (Figure 1; Supporting Information) for comparison. Crystals of **Pd1 a** and **Pd1 c** suitable for X-ray crystallography were obtained by diffusion of pentane or diethyl ether into dichloromethane solutions. Perspective views of the crystal structures are shown in Figure S2 (Supporting Information). The Pd–$C_{carbene}$ distances of **Pd1 a** and **Pd1 c** are 1.995 Å. Crystallographic and structural refinement data of **Pd1 a** and **Pd1 c** are summarized in Table S1–S6 (Supporting Information).

The UV/Vis absorption data and spectra of the $[Pd(C^N^N)(NHC)]^+$ complexes are depicted in Table S7, and Figures S3 and S4 (Supporting Information). Complexes **Pd1 a**–**Pd1 d** show strong absorption bands in

[*] Dr. T. T.-H. Fong, Dr. C.-N. Lok, Dr. C. Y.-S. Chung, Dr. Y.-M. E. Fung, Dr. P.-K. Chow, P.-K. Wan, Prof. Dr. C.-M. Che
State Key Laboratory of Synthetic Chemistry, Institute of Molecular Functional Materials and Department of Chemistry
The University of Hong Kong
Pokfulam Road, Hong Kong (China)
E-mail: cmche@hku.hk
Prof. Dr. C.-M. Che
HKU Shenzhen Institute of Research and Innovation
Shenzhen 518053 (China)

Supporting information for this article can be found under: http://dx.doi.org/10.1002/anie.201602814.

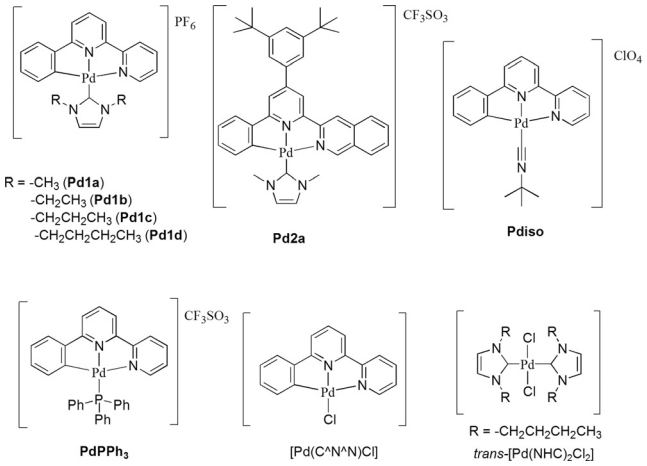

Figure 1. Chemical structures of the studied palladium complexes.

the region of 233–330 nm and a weaker absorption at approximately 383 nm, which are attributable to the intra-ligand (IL) transitions.

The stability of the palladium(II) complexes in the presence of biologically important thiols was examined. **Pd1b** (2 mM) in an aqueous buffer solution containing a mixture of ammonium bicarbonate (150 mM) and DMSO (4:1, v/v) was stable in the presence of a 10-fold excess of GSH (20 mM) at 40 °C and revealed no significant changes of the signals of **Pd1b** in the ^{1}H NMR spectrum for 24 h (Supporting Information, Figure S5a). In contrast, upon addition of excess GSH (20 mM) to **Pdiso** (2 mM) or **PdPPh$_3$** (4 mM), the ^{1}H NMR signals in the aromatic region (6–8.5 ppm) of **Pdiso** were different from those obtained without GSH (Supporting Information, Figure S6a), while the ^{31}P NMR signal of **PdPPh$_3$** revealed a significant change in chemical shift from 40 to −8 ppm (Supporting Information, Figure S6b). These findings suggest that, unlike the [Pd(C^N^N)(NHC)]$^+$ complexes, palladium(II) phosphine and isocyanide complexes undergo reactions readily with GSH. The solution stability of [Pd(C^N^N)(NHC)]$^+$ in the presence of GSH was further examined by electrospray ionization mass spectrometry (ESI-MS). A mixture of **Pd1a** (0.2 mM) and a 100-fold excess of GSH (20 mM) in aqueous buffer solution (50 mM ammonium bicarbonate, pH 7.6) was freshly prepared and the mass spectrum was recorded (Supporting Information, Figure S5b). The peak at $m/z =$ 433.3, corresponding to [**Pd1a**-PF$_6$]$^+$, was still observed after 24 h of incubation with GSH. In contrast, *trans*-[Pd(NHC)$_2$Cl$_2$] (0.2 mM) was found to react readily with GSH (20 mM) in pH 7.6 buffer solution, as revealed by the disappearance of the ion peak of *trans*-[Pd(NHC)$_2$Cl$_2$] ($m/z =$ 503.4) and the emergence of a [Pd(NHC)$_2$(GSH)]$^+$ adduct peak ($m/z = 772.3$) upon incubation with GSH for 1 h (Supporting Information, Figure S7). Additionally, the in vitro stability of **Pd1a** was also studied by LC-MS. No new peaks were found in the LC-MS chromatograms obtained from incubation of cell culture medium or HeLa cell extract with **Pd1a** (10 μM) for 48 h (Supporting Information, Figure S8). Furthermore, [Pd(C^N^N)(NHC)]$^+$ complexes were at least 5-fold less inhibitory toward thiol-dependent enzyme thioredoxin reductase compared to the thiol reactive **Pdiso** and **PdPPh$_3$** (Supporting Information, Table S8). We also investigated the reaction of **Pd1d** with a large excess of the non-thiol biological reductant, ascorbic acid. The absorption spectra of **Pd1d** did not show significant changes and ascorbic acid oxidation, as determined by monitoring of the absorbance at 265 nm, was not obvious for up to 24 h.

As serum albumin is known to strongly bind with and hence lower the bioavailability of drug molecules, the level of free palladium(II) complexes in the presence of human serum albumin (HSA) was examined with inductively coupled plasma mass spectrometry (ICP-MS) by measuring the amount of unbound palladium in a solution mixture of the complexes (2 μM) and HSA (60 μM; Supporting Information, Figure S9). It was found that more than 60% of **Pd1a** and 55% of **Pd1d** were left unbound after a 2 h incubation, while less than 16% of unbound palladium was found for other palladium(II) complexes. This suggests that [Pd(C^N^N)-(NHC)]$^+$ complexes have weaker interaction with HSA compared to other palladium(II) complexes. By protein fluorescence titration experiments, the binding constants of **Pd1a**, **Pd1d**, and **Pd2a** with HSA were determined to be $2.5(\pm 0.1)\times 10^5$, $4.7(\pm 0.3)\times 10^4$ and $1.8(\pm 0.2)\times 10^6\,\text{M}^{-1}$, respectively (Supporting Information, Figure S10).

The in vitro cytotoxicities of the palladium(II) complexes toward different human cancer cell lines, including a cervical epithelial cancer (HeLa), lung cancer (NCI-H1650 and NCI-H460), an aggressive triple-negative breast cancer (MDA-MB-231), and an ovarian cancer (A2780) and its cisplatin resistant clone (A2780cis) were investigated (Table 1). All the [Pd(C^N^N)(NHC)]$^+$ complexes were found to display promising antiproliferative activity toward the cancer cell lines with IC_{50} values of 0.09–2.5 μM, which were up to 172-fold more cytotoxic than cisplatin. The [Pd(C^N^N)(NHC)]$^+$ complexes displayed similar cytotoxicities in both A2780 and A2780cis, while cisplatin is relatively less cytotoxic (ca. 20-fold) toward cisplatin-resistant A2780cis compared to A2780. Notably, [Pd(C^N^N)(NHC)]$^+$ complexes were less cytotoxic toward a human normal lung fibroblast cell line (CCD-19Lu); for example, **Pd1d** showed an IC_{50} value of 11.8 μM toward CCD-19Lu, which is about 140-fold higher than that toward NCI-H1650 cells. On the other hand, other palladium-(II) complexes were found to show much lower cytotoxicity toward these cancer cells. This may be attributable to the aforementioned poor stability of these complexes in cellular conditions (Supporting Information, Figures S6 and S7) and their more significant binding with serum proteins (Supporting Information, Figure S9).

The involvement of apoptosis in the cytotoxic action of the [Pd(C^N^N)(NHC)]$^+$ complexes on cancer cells was examined. HeLa cells treated with **Pd1a** or **Pd1d** (0.5 μM) showed a dramatic increase in the cell population with reduced DNA content (sub-G1 phase in flow cytometry analysis; Supporting Information, Table S9), increases in the enzymatic activities of caspase-3 and caspase-9 (Supporting Information, Figure S11), and cleavage of PARP-1 (Supporting Information, Figure S12), signifying induction of apoptosis.

Table 1: In vitro cytotoxic IC_{50} values (μM, 72 h) of the palladium(II) complexes and cisplatin toward human cell lines of lung cancer (NCI-H1650 and NCI-H460), breast cancer (MDA-MB-231), cervical cancer (HeLa), ovarian cancer (A2780) and its cisplatin resistant clone (A2780cis), and normal lung fibroblast (CCD-19Lu).

Complex	IC_{50} [μM]]						
	NCI-H1650	NCI-H460	MDA-MB-231	HeLa	A2780cis	A2780	CCD-19Lu
Pd1a	2.5 ± 0.2	2.1 ± 0.2	0.9 ± 0.05	1.8 ± 0.1	2.2 ± 0.2	1.7 ± 0.2	32.1 ± 1.1
Pd1b	1.2 ± 0.09	1.1 ± 0.1	0.9 ± 0.06	1.4 ± 0.2	1.8 ± 0.2	1.5 ± 0.2	22.1 ± 1.9
Pd1c	0.5 ± 0.03	0.4 ± 0.05	0.8 ± 0.05	0.5 ± 0.05	1.2 ± 0.1	1.6 ± 0.1	15.4 ± 1.1
Pd1d	0.09 ± 0.01	0.08 ± 0.01	0.5 ± 0.06	0.1 ± 0.01	0.5 ± 0.05	0.2 ± 0.03	11.8 ± 1.2
Pd2a	0.9 ± 0.1	1.1 ± 0.09	0.4 ± 0.04	0.4 ± 0.03	2.5 ± 0.2	1.3 ± 0.2	8.9 ± 0.7
trans-$[Pd(NHC)_2Cl_2]$	> 100	> 100	> 100	> 100	> 100	> 100	> 100
[Pd(C^N^N)Cl]	> 100	> 100	> 100	> 100	> 100	> 100	> 100
$PdCl_2$	> 100	> 100	> 100	> 100	> 100	> 100	> 100
Pdiso	> 50	> 50	> 50	> 50	> 50	> 50	> 50
$PdPPh_3$	14.5 ± 1.2	15.2 ± 1.4	18.2 ± 1.7	11.2 ± 1.0	2.2 ± 0.1	3.2 ± 0.3	25.5 ± 2.1
cisplatin	15.5 ± 0.9	9.5 ± 0.8	20.5 ± 1.5	12.1 ± 1.1	30.5 ± 3.1	1.5 ± 0.1	95.5 ± 8.1

The cellular uptake of $[Pd(C^N^N)(NHC)]^+$ and other palladium(II) complexes was investigated by measuring palladium metal content in cell lysates using ICP-MS (Figure 2). Cancer cells (HeLa and NCI-H1650) were found to show 2-fold higher cellular uptake of $[Pd(C^N^N)(NHC)]^+$ complexes as compared to the normal CCD-19Lu cells. On the other hand, **$PdPPh_3$**, **Pdiso**, *trans*-$[Pd(NHC)_2Cl_2]$ and [Pd(C^N^N)Cl] all displayed much lower uptake into cancer and normal cells compared to that of $[Pd(C^N^N)(NHC)]^+$ complexes (with up to 50-fold difference; Figure 2). These findings highlight the unique structural features of $[Pd(C^N^N)(NHC)]^+$, which are important in the design of palladium medicines for cancer treatment.

The binding constants (K_b) for **Pd1a**, **Pd1d**, and **Pd2a** with calf-thymus DNA (ct DNA) determined from UV/Vis absorption data and Scatchard plots were found to be $14.2(\pm 0.8)\times 10^3$, $8.5(\pm 0.6)\times 10^3$, and $9.5(\pm 0.7)\times 10^3\,M^{-1}$, respectively (Supporting Information, Figure S13). The K_b values of **Pd1a**, **Pd1d**, and **Pd2a** are markedly lower than those of other palladium(II) complexes in the literature ($K_b \approx 10^{4-5}\,M^{-1}$),[6] and also the typical DNA intercalator ethidium bromide ($K_b \approx 10^7$), by up to several orders of magnitude. In a gel mobility shift assay, DNA ladder (123 bp) mixed with $[Pd(C^N^N)(NHC)]^+$ at a molar concentration equivalent to that of DNA base pairs did not show retarded mobility (Supporting Information, Figure S14). To examine whether $[Pd(C^N^N)(NHC)]^+$ complexes trigger DNA damage, such as double-strand breaks (DSBs) inside the cells, fluorescence microscopic examination of phosphorylated histone 2AX (γH2AX) was performed. γH2AX is an established marker for DSB, forming foci at the site of DNA breaks and appearing as punctate staining in the nucleus in immunofluorescence staining experiments.[7] It was found that HeLa cells displayed γH2AX foci after treatment with cisplatin for 24 h, but not with the $[Pd(C^N^N)(NHC)]^+$ complexes (Supporting Information, Figure S15). These results suggest that DNA is unlikely to be a major molecular target of $[Pd(C^N^N)(NHC)]^+$.

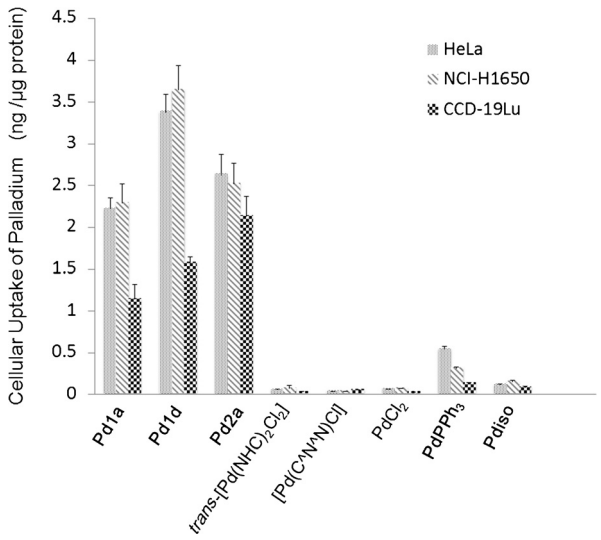

Figure 2. Cellular uptake of palladium, as quantified by ICP-MS. HeLa, NCI-H1650, and normal CCD-19Lu cells were treated with palladium complexes (5 μM) for 3 h.

As mitochondria is known to play key roles in activating cell apoptosis, the effect of **Pd1a** and **Pd1d** on mitochondria was investigated by a fluorescent probe of mitochondrial membrane potential, JC-1. HeLa cells treated with **Pd1a** or **Pd1d** (2.5 μM) for 2 h, followed by staining with JC-1, displayed green fluorescence, while orange fluorescence was observed in HeLa cells treated with solvent control (Supporting Information, Figure S16). The green fluorescence from cells treated with $[Pd(C^N^N)(NHC)]^+$ indicates disruption of the mitochondrial membrane potential by the complexes, which leads to cytosolic accumulation of green-emissive monomeric JC-1. To assess whether production of reactive oxygen species (ROS), which may be augmented owing to mitochondrial dysfunction, is involved in the $[Pd(C^N^N)(NHC)]^+$-induced cytotoxicity, HeLa cells were treated with **Pd1a** or **Pd1d** in the presence of excess cell permeable antioxidant *N*-acetylcysteine (NAC) and no significant change in cell viability was found (Supporting Information, Figure S17). These data are also consistent with the in vitro stability of $[Pd(C^N^N)(NHC)]^+$ in the presence of thiols.

A proteomic analysis of changes in protein expression mediated by **Pd1d** was performed using HPLC-LTQ-Orbitrap MS followed by computational pathway analysis.[8]

The lists of proteins (Supporting Information, Table S10) with expressions altered by **Pd1d** were uploaded to ExPlain™, which is connected to the BIOBASE database for upstream searching of keynodes for pathway and keynode analysis. Through the pathway analysis, it was found that 24 and 56 regulated pathways were identified from the HeLa cells treated with **Pd1d** for 2 h and 10 h, respectively (Supporting Information, Table S11). Many of these pathways were associated with apoptotic cell death and angiogenesis. Furthermore, the keynode network analysis[8] deduced that **Pd1d** acts on an upstream signaling pathway involving the growth factor receptor-bound protein 2 (Grb2), which is a key adaptor protein of diversified cancer-promoting growth factor receptors, such as epidermal growth factor receptor (EGFR) (Figure 3a).[9] To verify the effect of **Pd1d** on the EGFR signaling pathway, as implied by proteomic analysis, the EGF stimulated phosphorylation of EGFR and its downstream protein kinase ERK1/2 were studied by western blotting experiment (Figure 3b). Incubation of HeLa cells with **Pd1d** for 2 h led to significant decreases in phosphorylation of EGFR and ERK1/2 in a dose-dependent manner, suggesting that **Pd1d** inhibits EGFR signaling. Similar EGFR inhibition was also demonstrated in two lung cancer cell lines (NCI-H460 and HCC-827) under the same experimental conditions (Figure 3c and 3d).

The in vivo anticancer activity of **Pd1d** was examined. Nude mice bearing xenografts of NCI-H460 cancer cells were treated with **Pd1d** (1 mg kg^{-1} and 2 mg kg^{-1}) by intraperitoneal injection with eight repeated doses for 17 days. The treatment was found to inhibit tumor growth by 32% ($p < 0.05$) and 61% ($p < 0.05$), respectively, as compared to those treated with a solvent control (Figure 4a). Importantly, no mouse death or significant body weight loss was found after the treatment with **Pd1d** at these doses (Figure 4b). At the end of the experiments (two days after the last compound administration), mice were sacrificed and the in vivo levels of **Pd1d** were studied by LC-MS/MS. Intact cation of **Pd1d** was found in the tumor (0.048 ± 0.015 μg g^{-1} of tissue) and blood plasma (9 ± 3 nM; Supporting Information, Figure S18). The in vivo anticancer activity of **Pd1d** was also examined in nude mice bearing xenografts of HeLa cancer cells; **Pd1d** (1 mg kg^{-1} and 3 mg kg^{-1}) was administered by intraperitoneal injection with seven repeated doses for 13 days. Treatment was found to inhibit tumor growth by 40% ($p < 0.05$) and 55% ($p < 0.05$), respectively, as compared to those treated with solvent control (Supporting Information, Figure S19). Furthermore, the anticancer properties of [Pd(C^N^N)(NHC)]$^+$ complexes were investigated in terms of their anti-angiogenic activities. Incubation of mouse endothelial cells (MS1) with **Pd1a** and **Pd1d** at sub-cytotoxic concentrations (0.25 μM and 0.5 μM) resulted in distortion of the endothelial tube formation in Matrigel (Supporting Information, Figure S20a) and cell migration in wound healing assay (Supporting Information, Figure S20b).

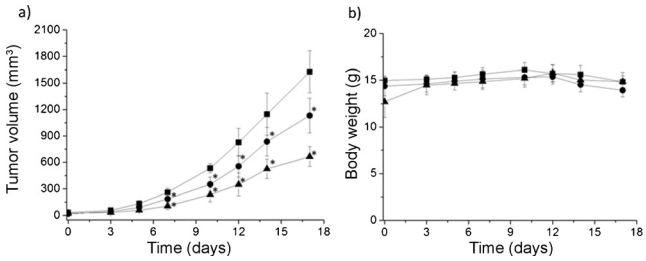

Figure 4. a) Average tumor volumes of NCI-H460 xenograft-bearing mice treated with solvent or **Pd1d** through intraperitoneal injection of eight repeated doses for 17 days. Error bars represent standard deviations, $n = 5$, * denotes $p < 0.05$ compared to solvent control. b) Body weight of mice in different groups. Key: solvent control (—■—), **Pd1d** (1 mg/kg; (—●—)), **Pd1d** (2 mg/kg; (—▲—)). The x-axes depict days after the first **Pd1d** injection.

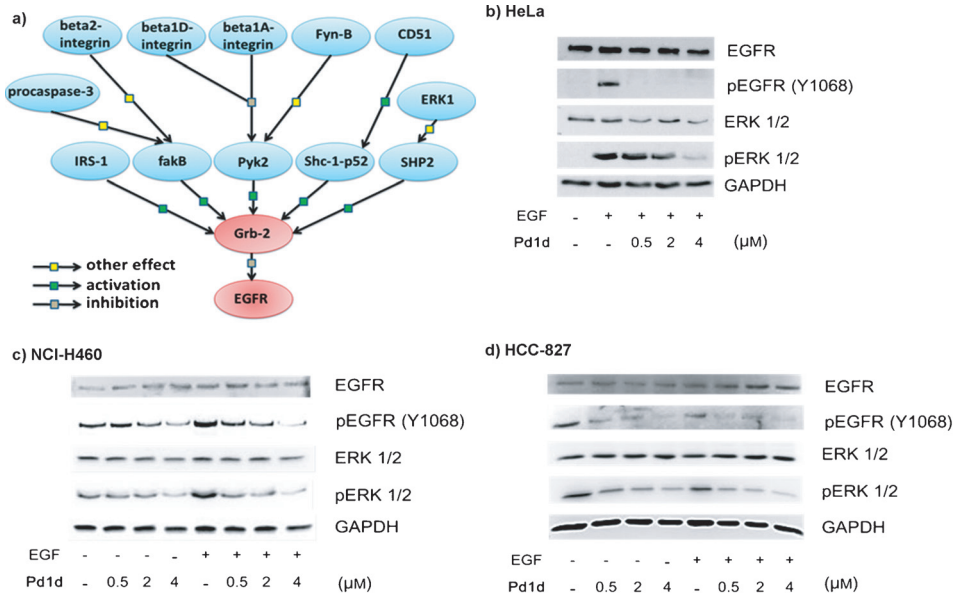

Figure 3. a) Keynode network analysis of proteomic data obtained from HeLa cells treated with **Pd1d** indicated that **Pd1d** acts on the EGFR/Grb2 pathway. b–d) Inhibitory effect of **Pd1d** on EGFR signaling. Cancer cells were treated with the indicated concentrations of **Pd1d** for 2 h. After EGFR stimulation with EGF (50 ng mL^{-1}) for 15 min, cells were harvested and lysed, and the activation/phosphorylation of EGFR (pEGFR) and its downstream protein kinase (pERK) were analyzed by western blotting technique. (b) HeLa cervical cancer cells, (c) NCI-H460 lung cancer cells, (d) HCC-827 lung cancer cells.

In summary, [Pd(C^N^N)(NHC)]$^+$ complexes demonstrate high stability in vitro and in the presence of physiological thiols. The complexes show potent in vitro cytotoxicities against cancer cells, as well as effective in vivo anticancer activities toward tumor xenograft in nude mice, with no observable toxicity. The mechanism of anticancer action of the complexes, as investigated by

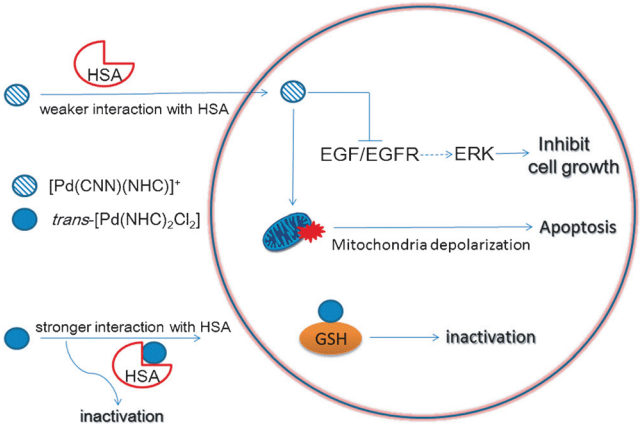

Figure 5. Proposed anticancer mechanisms for action of [Pd(C^N^N)(NHC)]$^+$.

proteomics analysis and biochemical assays, involved induction of mitochondrial dysfunction and inhibition of EGFR signaling pathway in association with apoptotic cell death of the cancer cells (Figure 5). The present work highlights the promising prospects of NHC and pincer-type cyclometalated ligands in the development of palladium(II) complexes for anticancer treatment.

Acknowledgements

This work was supported by the Innovation and Technology Fund (ITF-Tier 2, ITS/130/14FP) administered by the Innovation and Technology Commission, General Research Fund (HKU 700812P and HKU17300614) from Research Grants Council, Area of Excellence Scheme (AoE/P-03/08) of the University Grants Committee and the National Key Basic Research Program of China (2013CB834802). We thank Chen Yang for great assistance in X-ray crystal structure determinations, I-Sheng Chang for help in proteomic pathway analysis, and Dr. Taotao Zou for constructive comments.

Keywords: anticancer agents · N-heterocyclic carbenes · palladium · proteomics · thiol reactivity

How to cite: *Angew. Chem. Int. Ed.* **2016**, *55*, 11935–11939
Angew. Chem. **2016**, *128*, 12114–12118

[1] a) J. Xuan, T.-T. Zeng, Z.-J. Feng, Q.-H. Deng, J.-R. Chen, L.-Q. Lu, W.-J. Xiao, H. Alper, *Angew. Chem. Int. Ed.* **2015**, *54*, 1625; *Angew. Chem.* **2015**, *127*, 1645; b) P.-K. Chow, W.-P. To, K.-H. Low, C.-M. Che, *Chem. Asian J.* **2014**, *9*, 534; c) J. C. Bernhammer, N. X. Chong, R. Jothibasu, B. Zhou, H. V. Huynh, *Organometallics* **2014**, *33*, 3607; d) S. L.-F. Chan, R. W.-Y. Sun, M.-Y. Choi, Y. Zeng, L. Shek, S. S.-Y. Chui, C.-M. Che, *Chem. Sci.* **2011**, *2*, 1788; e) E. A. B. Kantchev, C. J. O'Brien, M. G. Organ, *Angew. Chem. Int. Ed.* **2007**, *46*, 2768; *Angew. Chem.* **2007**, *119*, 2824.

[2] a) J.-Y. Lee, J.-Y. Lee, Y.-Y. Chang, C.-H. Hu, N. M. Wang, H. M. Lee, *Organometallics* **2015**, *34*, 4359; b) N. Miklášová, E. Fischer-Fodor, R. Mikláš, L. Kucková, J. Kožíšek, T. Liptaj, O. Soritau, J. Valentová, F. Devínsky, *Inorg. Chem. Commun.* **2014**, *46*, 229; c) A. R. Kapdi, I. J. S. Fairlamb, *Chem. Soc. Rev.* **2014**, *43*, 4751; d) E.-J. Gao, H. Fu, M.-C. Zhu, C. Ma, S.-K. Liang, J. Zhang, L.-F. Li, L. Wang, Y.-Y. Li, W. Jiao, *Eur. J. Med. Chem.* **2014**, *82*, 172; e) N. Cutillas, G. S. Yellol, C. de Haro, C. Vicente, V. Rodriguez, J. Ruiz, *Coord. Chem. Rev.* **2013**, *257*, 2784; f) E. J. Gao, M. Zhu, H. Yin, L. Liu, Q. Wu, Y. Sun, *J. Inorg. Biochem.* **2008**, *102*, 1958; g) S. Ray, R. Mohan, J. K. Singh, M. K. Samantaray, M. M. Shaikh, D. Panda, P. Ghosh, *J. Am. Chem. Soc.* **2007**, *129*, 15042; h) A. S. Abu-Surrah, M. Kettunen, *Curr. Med. Chem.* **2006**, *13*, 1337; i) F. L. Wimmer, S. Wimmer, P. Castan, S. Cros, N. Johnson, E. Colaciorodrigez, *Anticancer Res.* **1989**, *9*, 791.

[3] a) T. Zou, C. T. Lum, C.-N. Lok, J.-J. Zhang, C.-M. Che, *Chem. Soc. Rev.* **2015**, *44*, 8786; b) C.-M. Che, F.-M. Siu, *Curr. Opin. Chem. Biol.* **2010**, *14*, 255.

[4] a) M. N. Hopkinson, C. Richter, M. Schedler, F. Glorius, *Nature* **2014**, *510*, 485; b) M. V. Baker, P. J. Barnard, S. J. Berners-Price, S. K. Brayshaw, J. L. Hickey, B. W. Skelton, A. H. White, *Dalton Trans.* **2006**, 3708; c) W. A. Herrmann, C. Kocher, *Angew. Chem. Int. Ed. Engl.* **1997**, *36*, 2162; *Angew. Chem.* **1997**, *109*, 2256.

[5] a) R. W.-Y. Sun, A. L.-F. Chow, X.-H. Li, J. J. Yan, S. S.-Y. Chui, C.-M. Che, *Chem. Sci.* **2011**, *2*, 728; b) J. J. Yan, A. L.-F. Chow, C.-H. Leung, R. W.-Y. Sun, D.-L. Ma, C.-M. Che, *Chem. Commun.* **2010**, *46*, 3893; c) P. Wang, C.-H. Leung, D.-L. Ma, W. Lu, C.-M. Che, *Chem. Asian J.* **2010**, *5*, 2271.

[6] a) C. Icsel, V. T. Yilmaz, *DNA Cell Biol.* **2013**, *32*, 165; b) E. Ramachandran, D. S. Raja, N. S. P. Bhuvanesh, K. Natarajan, *Dalton Trans.* **2012**, *41*, 13308; c) M. Cusumano, M. L. Di Pietro, A. Giannetto, P. A. Vainiglia, *Eur. J. Inorg. Chem.* **2005**, 278.

[7] L. J. Kuo, L.-X. Yang, *In Vivo* **2008**, *22*, 305.

[8] a) S.-T. Lau, T. Zhou, J. A.-J. Liu, E. Y.-M. Fung, C.-M. Che, B. H.-H. Lang, E. S.-W. Ngan, *Biochim. Biophys. Acta Mol. Basis Dis.* **2015**, *1852*, 1676; b) H. K. Nyblom, M. Bugliani, E. Fung, U. Boggi, R. Zubarev, P. Marchetti, P. Bergsten, *J. Proteome Res.* **2009**, *8*, 5650; c) R. A. Zubarev, M. L. Nielsen, E. M. Fung, M. M. Savitski, O. Kel-Margoulis, E. Wingender, A. Kel, *J. Proteomics* **2008**, *71*, 89; d) S. Stahl, E. Fung, C. Adams, J. Lengqvist, B. Mork, B. Stenerlow, R. Lewensohn, J. Lehtio, R. Zubarev, K. Viktorsson, *Mol. Cell. Proteomics* **2009**, *8*, 1117.

[9] a) A. Tomas, C. E. Futter, E. R. Eden, *Trends Cell Biol.* **2014**, *24*, 26; b) A. A. Belov, M. Mohammadi, *Sci. Signaling* **2012**, *5*, pe49.

Received: March 21, 2016
Revised: June 15, 2016
Published online: August 29, 2016

